AFFDL-TR-77-38

12
NL

COMPARISON OF EXPERIMENT AND ANALYSIS FOR A HIGH PRIMARY MACH NUMBER EJECTOR

THERMOMECHANICS BRANCH
AEROMECHANICS DIVISION

MAY 1977

TECHNICAL REPORT AFFDL-TR-77-38
INTERIM REPORT FOR PERIOD SEPTEMBER 1975 to OCTOBER 1976

AIR FORCE FLIGHT DYNAMICS LABORATORY
AIR FORCE WRIGHT AERONAUTICAL LABORATORIES
AIR FORCE SYSTEMS COMMAND
WRIGHT-PATTERSON AIR FORCE BASE, OHIO 45433

NOTICE

When Government drawings, specifications, or other data are used for any purpose other than in connection with a definitely related Government procurement operation, the United States Government thereby incurs no responsibility nor any obligation whatsoever; and the fact that the government may have formulated, furnished, or in any way supplied the said drawings, specifications, or other data, is not to be regarded by implication or otherwise as in any manner licensing the holder or any other person or corporation, or conveying any rights or permission to manufacture, use, or sell any patented invention that may in any way be related thereto.

This report has been reviewed by the Information Office (ASD/OIP) and is releasable to the National Technical Information Service (NTIS). At NTIS it will be available to the general public, including foreign nations.

This technical report has been reviewed and is approved for publication.

Siegfried H. Hasinger
Aerospace Engineer

ALFRED C. DRAPER
Asst for Research & Technology
Aeromechanics Division

Copies of this report should not be returned unless return is required by security considerations, contractual obligations, or notice on a specific document.

AIR FORCE - 20 JUN 77 - 150

UNCLASSIFIED

SECURITY CLASSIFICATION OF THIS PAGE *(When Data Entered)*

REPORT DOCUMENTATION PAGE		READ INSTRUCTIONS BEFORE COMPLETING FORM
1 REPORT NUMBER AFFDL-TR-77-38	2. GOVT ACCESSION NO.	3 RECIPIENT'S CATALOG NUMBER
4. TITLE *(and Subtitle)* Comparison of Experiment and Analysis for a High Primary Mach Number Ejector,		5 TYPE OF REPORT & PERIOD COVERED Interim Report, Sept. 1975 — Oct. 1976,
		6. PERFORMING ORG. REPORT NUMBER
7. AUTHOR(s) Siegfried H. Hasinger Earnest F. Fretter		8. CONTRACT OR GRANT NUMBER(s)
9. PERFORMING ORGANIZATION NAME AND ADDRESS Thermomechanics Branch Air Force Flight Dynamics Laboratory Wright-Patterson Air Force Base, Ohio 45433		10 PROGRAM ELEMENT, PROJECT, TASK AREA & WORK UNIT NUMBERS Project No. - 2307 Task No. - 230704 Work Unit No. - 23070426
11. CONTROLLING OFFICE NAME AND ADDRESS Air Force Flight Dynamics Laboratory Wright-Patterson Air Force Base, Ohio 45433		12. REPORT DATE May 1977 13. NUMBER OF PAGES 56 (+ 60 p.)
14. MONITORING AGENCY NAME & ADDRESS *(if different from Controlling Office)*		15. SECURITY CLASS. *(of this report)* UNCLASSIFIED 15a. DECLASSIFICATION/DOWNGRADING SCHEDULE N/A

16 DISTRIBUTION STATEMENT *(of this Report)*

Approved for public release; distribution unlimited

17. DISTRIBUTION STATEMENT *(of the abstract entered in Block 20, if different from Report)*

18. SUPPLEMENTARY NOTES

19. KEY WORDS *(Continue on reverse side if necessary and identify by block number)*

Ejector Performance
Supersonic Ejector
Ejector Optimization
Ejector Analysis
Ejector Experiments

20. ABSTRACT *(Continue on reverse side if necessary and identify by block number)*

Analytical predictions derived from ARL TR-75-0205 are compared with test results for two ejectors which have the same inlet geometry; however, one has a constant area mixing section and no subsonic diffuser, while the other has a tapered mixing section, a constant area supersonic diffuser and a subsonic diffuser. The purpose of the first configuration is to provide well defined experimental conditions for the comparison of analysis and experiment, while the second configuration is designed to give optimum

DD FORM 1 JAN 73 1473 EDITION OF 1 NOV 65 IS OBSOLETE

UNCLASSIFIED

SECURITY CLASSIFICATION OF THIS PAGE *(When Data Entered)*

012070

performance. The design goal in this case is a total ejector pressure ratio of five at a mass flow ratio (primary to secondary) of five. For both ejector configurations the experiments agreed very satisfactorily with the analysis. However, some ambiguity is involved in the predictions for the optimized ejector. This is due to the difficulties in predicting the pressure distribution during mixing. The present experiments make it apparent that the optimum performance is inherently connected with a near constant pressure distribution. More testing is necessary to confirm this result. Should it hold, ejector optimization could be made more reliable. For the present comparison the analysis of ARL TR 75-0205 is extended to include off-design conditions for the primary supersonic ejector nozzles.

FOREWORD

This investigation was carried out under Work Unit No. 2307Ø426 of Project 2307 in the Thermomechanics Branch, Aeromechanics Division, Flight Dynamics Laboratory, from September 1975 to October 1976, as a logical follow-on to the investigations reported in ARL TR-75-0205, "Performance Characteristics of Ejector Devices", June 1975.

The authors would like to thank Capt. David K. Miller, Technical Manager, Gas Energetics Group, Thermomechanics Branch, for his support and his valuable suggestions for carrying out the present experiments. We highly appreciate Mr. Howard Toms' expertise in designing the test facility and directing its installation. Special thanks go to Mr. Marion D Linder and Mr. Mont Ball for their continuing cooperation and excellent workmanship in fabricating the ejector apparatus from often sketchy design drawings and to Mr. Stan Pettigrew for his invaluable help in installing and operating the test facility.

TABLE OF CONTENTS

LIST OF ILLUSTRATIONS

LIST OF SYMBOLS

a	speed of sound
A	flow cross-sectional area
c_f	wall friction coefficient
D	mixing section diameter
i	pressure distribution factor, see Section IV 3
L	reference length for wall friction
$\dot{m}$	mass flow rate
M	flow Mach number
p	static pressure
T	absolute static temperature
t	flow cross-sectional area reduction of mixing section $= A_{Ex}/(A_p + A_s)$
v	flow velocity
γ	ratio of specific heats
η_{pol}	polytropic subsonic diffuser efficiency

INDICES

Ex	refers to mixing section exit
geo	refers to given geometric design conditions
noz	refers to geometric exit of the primary nozzle
p	refers to the primary air flow
s	refers to the secondary air flow
$( )_o$	refers to stagnation conditions

SECTION I

INTRODUCTION

The primary purpose of the present experiments is to check the validity of the ejector analysis reported in Ref. 1. This analysis treats gaseous ejectors for highly compressible operating media. Its aim was a generalized presentation of the performance behavior of ejectors and various simplifications were introduced. In particular, one dimensional flow was assumed. Since the analysis should be useful for practical design purposes the effect of these simplifications on the practical reliability of the analysis needs to be checked.

The present experiments are desirable for other reasons. The analysis considers only design point performance, i.e., in the case of supersonic primary Mach numbers it assumes that the primary nozzle has the correct area expansion. Within certain limits the performance is affected only slightly by off-design conditions. It is of practical interest to know these limits and to find ways to account for off-design effects. The present experiments provide an occasion to study this off-design problem.

Although the analysis is able to account for any assumed static pressure distribution during mixing, it cannot predict the pressure distribution itself. The pressure distribution during mixing is an important factor for an ejector with a tapered mixing section, since with the right pressure distribution such a mixing section can sub-

stantially improve the ejector performance. The prediction of the pressure distribution in an ejector with at least one supersonic component is an unsolved problem and experiments become the only reliable source of information in this case.

SECTION II

SCOPE OF THE EXPERIMENTS

The design goal for the present ejector experiments was a total ejector pressure ratio (total exit pressure to secondary plenum pressure) of 5. This performance was considered typical for a high Mach number ejector. An ejector of this rating with air as operating media was designed in accordance with the optimization procedure given in Reference 1, featuring a reducing area mixing section. This optimized design was actually tested and results are given in this report. However, the bulk of the experiments reported were carried out with a modified version of the above design to simplify the comparison with the analysis.

Two modifications were made: The ejector was given a constant area mixing section and the subsonic diffuser was eliminated. The mixing section was made long enough to always assure complete mixing of primary and secondary flows. It is obvious that a subsonic diffuser becomes irrelevant under these circumstances to the basic functioning of the ejector. With this modified ejector the performance is derived from the static pressure peak occurring in the mixing section. The experiments with this ejector, referred to in the following as the "basic ejector," provided a frame of reference for dealing with the more complex flow mechanism of the optimized ejector.

To increase the range of operating conditions, a primary nozzle

for Mach number 2.7 was also used in addition to the original primary nozzle designed for Mach number 3.2 for the optimized ejector. Both nozzles have the same throat cross-sectional area.

A mixing section with a constant area square cross-section was also investigated. All experiments with the basic and the optimized ejector were carried out with the ejector discharging to ambient.

SECTION III

EXPERIMENTS WITH THE BASIC EJECTOR

1. Apparatus

The ejector was tested with both a round and a square mixing section. In the first case it consisted of a constant area plexiglass tube with a diameter of 1.5" (3.81cm) as shown in Figure 1. The upstream end has a bell mouth inlet geometry with a contour radius of about 1" (2.54cm). Pressure taps of .041" (.104cm) are drilled into the tube every 1/2" (1.27cm) from the end of the bell mouth to 17" (43.2cm) downstream, then every inch (2.54cm) thereafter to 30" (76.2cm) from the plenum chamber.

The square shaped mixing section, which was used to determine the influence of the cross-section shape on the ejector performance, was also provided with a bell mouth inlet and had nominally the same cross-sectional areas as the round mixing section. The exact side lengths of the square cross section were 1.319" (3.45cm) x 1.319" (3.45cm). The total length of the section was 29.94" (76cm). The arrangement of the pressure taps was the same as the one for the round section.

The nozzles used for the experiments are shown in Figure 2. They are identified as the M2.7 nozzle and M3.2 nozzle, with exit Mach numbers of 2.7 and 3.28 corresponding to their actual area expansion ratios.

The supersonic nozzles were not designed to provide a true

parallel exit flow and had instead a simple conical contour for the expanded portion of the nozzle. However, the cone angle was kept within 10°, small enough to minimize the effects of deviations from a parallel flow nozzle (See Section III 5).

The position of the nozzle exit plane could be varied from 1.5" (3.82cm) inside the mixing duct to 3 1/2" (8.9cm) upstream inside the secondary plenum chamber. Tests proved that the ejector performance is, within certain limits, not very sensitive to the axial position of the primary nozzle in respect to the bell mouth inlet. Most of the tests were, therefore, carried out with one judiciously chosen position. This position provided for the nozzle exit plane to be located about 1/2" (1.27cm) upstream of the point where the constant area cross-section of the mixing tube begins. This position was far enough upstream with respect to the bell mouth inlet to assure an unrestricted and continuously accelerating secondary flow. The position was also close enough to the entrance of the actual mixing tube (beginning of the constant cross-sectional area) to allow a proper identification of the primary to secondary inlet area ratio as derived from the primary jet diameter and the mixing section diameter. The analytical determination of the primary jet diameter for off-design conditions, i.e., for primary Mach numbers larger than design Mach number, is given in the Appendix.

A special effort was made to align the primary nozzle coaxially with the mixing section. This was first done geometrically and then checked by the uniformity of the static pressure at three positions

uniformly spaced around the periphery of the mixing section inlet. It was never possible to obtain complete uniformity of the static pressure at these positions. In addition the degree of uniformity depended on the operating conditions. However, the ejector performance was not very sensitive to the degree of the static pressure uniformity and deviations on the order of 10% were tolerated at higher secondary flow rates. At very low secondary flow rates, approaching zero secondary flow, a considerable non-uniformity of the static pressures at the inlet existed. Dynamic pressure measurement showed that in this case the non-uniformity was caused by asymmetric recirculation in the inlet area.

The secondary plenum chamber is a cylindrical container 4" (10.2cm) in diameter and 5" (12.7cm) in length. Three static pressure taps and one thermocouple are located around the periphery of the chamber.

Figure 3 schematically illustrates the general arrangement of the experiment. The air supply is from the building bottle farm, reduced to 500 psig (35.2kg/cm^2 gage) working pressure at the test site. Heated typically to 70°F (21°C) before entering the test rig, the primary air supply was regulated from 0 to 200 psig (0 to 14.1kg/cm^2 gage) for typical test conditions.

The secondary mass flow was controlled by five separate, sonic orifices upstream of the plenum chamber. Any combination of the five mass flow orifices could be used to give any desired secondary mass flow from zero to .441 lb/sec (.2kg/sec), depending on the or-

ifice chosen and the secondary supply pressure.

2. Instrumentation

Standard laboratory instrumentation was used to measure total temperature, supply pressure, primary and secondary total pressure, and the secondary supply pressure to the mass flow control valves.

Two Statham model PG769, 0-200 (0-14.1) and 0-100 psig (0-7.05 kg/cm^2 gage) transducers were used to measure primary total pressure and secondary supply pressure respectively. The signals were recorded on a Hewlett Packard (HP) model 2FA X, Y, Y' plotter. A Statham model PM397C $\pm$ 300" (762cm) H_2O transducer was used to measure the secondary total pressure, also recorded on the HP plotter. A 30" (76.2cm) mercury manometer was used to measure directly the secondary total pressure (secondary plenum pressure) at the control console and ambient pressure was read from a mercury barometer.

The differential pressure between the mixing section inlet (beginning of the constant area section) and the secondary plenum was measured with 60" (152cm) flexible U-tube water manometers ("slack tube manometers") at 3 locations (at 4 locations for the square tube) around the periphery of the mixing tube inlet. All wall static pressures along the mixing tube were scanned by a Scanivalve model SSS48C4BM, using a Statham $\pm$ 15 psia ($1.05 kg/cm^2$) pressure transducer. These signals were fed to one channel of an S. Sterling Co. data acquisition system. Another channel received a signal from a port-positioning sensor. Both signals then give a

pressure-position trace on a strip chart recorder of the system.

The total temperatures of the primary and the secondary air flow as well as the temperature of the air exiting the heater were measured by grounded, fast response iron-constant thermocouples whose signals were read from Simplytrol pyrometers on the control console.

3. Testing Procedure

The pressure and mass flows for each run were adjusted for either a constant mass ratio or a constant pressure ratio condition, usually the latter. For the secondary flow, the flow control orifice was selected which gave a supply pressure range from 0-100 psig (0-7.05 kg/cm^2).

For a constant pressure ratio run, the required secondary plenum pressure was calculated from the given ejector pressure ratio and the expected pressure peak in the mixing section, which was in general very near ambient pressure. The peak pressure was then experimentally checked at typical run conditions and the secondary plenum pressure recalculated if necessary. Then, the primary and secondary supply pressure were readjusted to give the required total secondary pressure reading on the mercury manometer. Heat was added to keep the air streams at or near 70°F (21.1°C) during a test run. Once the temperatures and pressures of the primary and secondary flows were stabilized, a Scanivalve trace was taken and the data recorded from the control panel, slack tube manometers, and from the X, Y,

Y' plotter. For subsequent test points, the primary and the secondary pressure were readjusted to give the same total secondary pressure but at a different mass ratio.

For a constant mass ratio run the primary and the secondary supply pressure (X and Y coordinates of the plotter) were adjusted to keep the pen trace of the plotter on a given straight line through the zero point of the coordinate system. Since the primary mass flow is proportional to the primary supply pressure due to the supersonic condition in the primary nozzle and the secondary flow proportional to the secondary supply pressure due to the sonic condition at the orifice valve, a straight line through the zero point of the coordinate system represents a line of constant mass flow ratio.

Pressure transducers were calibrated at least daily against a precision Heise gauge. Thermocouples were calibrated at two points, in an ice bath, and in boiling water.

The initial data was transcribed onto data sheets. The Scanivalve tracing was used to obtain pressure-position information as well as the maximum pressure inside the duct, P_{ex}. The X, Y, Y' plotter graph gave secondary supply pressure (used to calculate the secondary mass flow rate) and secondary total pressure. The slack tube manometer data gave an accurate reading of the average secondary pressure at the beginning of mixing against the secondary plenum pressure.

4. Results

Figures 4 and 5 show a comparison of the experimental and analytical performance of the basic ejector as described in Section II. Figure 4 gives the performance for the Mach number 2.7 primary nozzle and Fig. 5 gives the performance for the Mach number 3.2 primary nozzle with the ejector geometry otherwise unchanged.

The type of performance characteristics shown in these figures was developed in Ref. 1. In these characteristics the secondary inlet Mach number is plotted against the primary Mach number with the total pressure ratio (total exit pressure over secondary plenum pressure) and ejector mass flow ratio appearing as curve parameters. The absence of a subsonic diffuser in the present case is accounted for by assuming the subsonic diffuser efficiency to be zero. This assumption also means that the total exit pressure can be replaced by the static pressure. Fig. 6 gives the ejector pressure ratio in terms of the absolute primary and secondary mass flows for the Mach number 2.7 primary nozzle.

Input data for the analysis are as follows:

Ratio of the primary to secondary flow cross section area at the location of the primary nozzle exit

$$(A_p/A_s)_{geo} = .28 \text{ for the M2.7 nozzle}$$
$$= .62 \text{ for the M3.2 nozzle}$$

Plenum temperature ratio (primary to secondary):

$$(T_p)_o/(T_s)_o = 1.0$$

Actually temperature differences of about 2° to 4°F (1.1° to 2.2°C) occurred. Typical operating temperatures were 70° (21.1°C) primary flow, 68°F (20°C) secondary flow. Subsonic diffuser efficiency (polytropic efficiency):

$$\eta_{pol} = 0$$ (the zero value accounts for the absence of a subsonic diffuser)

Wall friction factor:

$$c_f \cdot L/(2D) = .12$$

This value was maintained constant throughout the characteristics shown in Figures 4 and 5. The experiments showed that the mixing length (L) occurring in this factor did change to some degree with the operating conditions (not considering for the moment the mixing mode change to be discussed in Section III 6). Discrepancies between experimental and analytical values can in part be traced to inaccurate mixing length assumptions in the analysis.

The wall friction factor was determined in a special flow experiment in which only secondary air was supplied to the ejector mixing section. From the pressure drop along the mixing section a wall friction coefficient of .024 was derived. At a Reynolds number of 10^5 typical for the test this friction coefficient value is higher than one could expect for the smooth plexiglas tube used. The difference has been attributed to the fact that in the present determination the flow was not fully developed. In view of the uncertainties involved in the character of the actual ejector flow it

was not found useful to determine a more accurate friction coefficient. The length L required for mixing was assumed to be 10 mixing section diameters. The experiments confirmed this value as a good average.

The analysis allows one to use either the primary, secondary, or mixing section exit Mach number as a reference Mach number for determining the wall friction (see Ref. 1). In the present case the mixing section exit Mach number is used for reference.

The primary supply tube, which acted as the plenum for measuring the total primary supply pressure, had a diameter 2.6 times larger than the throat of the primary nozzles used in the experiments. The resulting approach Mach number in the supply tube was about .08 in the cases of interest. To account for the approach Mach number, the pressure ratio by which the measured pressure ratio would have to be divided is .995. This gain in pressure ratio is of the same order of magnitude as the loss caused by wall friction in the primary nozzle. For the present evaluation it was assumed that both effects cancel each other, i.e., these effects have been neglected.

To enter a test point in the characteristic of Fig. 4 or 5 the following procedure was applied: The primary Mach number M_p is determined from Eq. 14 (see Appendix) by entering the experimentally found ratio of primary supply pressure to static pressure at the mixing section inlet. All other magnitudes occurring in the equation are given by the primary nozzle lay-out. Then the mass flow

ratio is determined from the ratio of the primary to the secondary supply pressure, together with the ratio of the primary nozzle throat area to the area of the orifice of the selected supply valve and the temperature ratio between primary and secondary flow.

With the primary Mach number and the mass flow ratio known the test point can be plotted on the characteristic. Instead of doing the plotting graphically by interpolating between the mass flow ratio curves, the primary Mach number and the mass flow ratio found for a test point were used as input to the analysis. With the basic geometry of the ejector given, the analysis then yields the secondary Mach number and the ejector pressure ratio. An automatic plotter was used to enter the test point in the characteristic.

The secondary Mach number and the ejector pressure ratio resulting from plotting of the test point can now be compared with actually measured values. However, only the pressure ratio is given exactly from the experiments. For the test points in Figs. 4 and 5 the total pressure ratios have been very carefully maintained to be at the even values of 4, 5, 6, and 7, within less than $\pm$ 1%. Thus analysis and experiment agree completely if the test point falls on the corresponding pressure ratio lines in Figs. 4 and 5. The present results indicate that the agreement is in general quite satisfactory. Details of the comparison will be discussed in Sect. III 5. The role of the secondary Mach number in the comparison will be explained next.

Of the four magnitudes which can be derived from the experiment:

Mass flow ratio, primary Mach number, total pressure ratio, and secondary Mach number, the latter one is the least reliable. This is due to a certain lack of flow uniformity at the ejector inlet and in some cases a lack of definition for the pressure conditions at the inlet.

The secondary Mach number follows directly from the ratio of secondary plenum pressure to static pressure at the point in the mixing section where the primary flow is fully expanded. This point is not given exactly. However, for the flow conditions prevailing for the test points in Figs. 4 and 5, the static pressure remains constant for at least a length of 2 mixing tube diameters, as can be seen from Fig. 7 for the curves 1 to 3, which represent pressure distributions typical for the test points in Figs. 4 and 5. From general experience with the flow pattern for off-design nozzles, it is obvious that the primary flow is fully expanded within this length. Thus, in these cases the static pressure prevailing at the beginning of the mixing section is a fairly reliable basis for determining the secondary Mach number. The difficulty is, as mentioned before, that the wall pressure in the inlet region is not completely uniform over the periphery. In the present evaluation an average value of the water manometer reading (differential pressure between secondary plenum and inlet static pressure) taken around the periphery was taken as static inlet pressure. The secondary Mach numbers derived from these readings agree with those found from Figs. 4 and 5 within about $\pm$ 3%, being in general on the positive side.

For the conditions where the mixing mode has changed to supersonic conditions as explained in more detail in Sect III 6, the static inlet pressure can no longer be directly read from the pressure distribution curves. As Fig. 7 shows for the curves 5 and 6, which are representative for the supersonic mode of mixing, the pressure drops continuously in the inlet region for a length of up to 4 mixing diameters. This is more length than needed for the primary flow to expand to the pressure level of the secondary flow. Thus it must be assumed that the pressure in the mixing section continues to drop even after the primary flow has reached the pressure level of the secondary flow. Due to this continued drop in pressure, the pressure distribution curve itself does not signify the point where primary and secondary pressure become equal.

An approximate value of the secondary Mach number is known from plotting the test point in Figs. 4 or 5. This value can be used to determine the pressure level to which the secondary flow must expand to achieve this Mach number.

Such determinations have been made. They confirm that the pressure in the mixing section continues to drop after the primary flow has expanded to the pressure of the secondary flow. Thus, mixing, at least for a while, apparently takes place at decreasing pressure.

The above method of determining the ejector inlet pressure was used in calculating the primary Mach number in the case of supersonic mixing. Since the determination of the secondary Mach number

requires the knowledge of the primary Mach number, a final result can only be obtained by iteration. This iteration is not very sensitive to the assumptions about the secondary Mach number.

5. Discussion of the Results

Experiment and analysis agree quite well for the Mach number 2.7 nozzle. There is practically no difference in the agreement for the round and square mixing section. For the Mach number 3.2 nozzle the required primary Mach number is consistently somewhat above the calculated value with the discrepancy increasing with the ejector pressure ratio. One possible cause is the flow quality of the primary nozzle, which due to its conical contour produces a radial component which is of no value in the injection process. This effect must increase with the portion of the expansion taking place in the supersonic part of the nozzle, i.e., the effect should be more pronounced with the higher Mach number nozzle. Also the boundary layer along the nozzle wall must increase with the length of the nozzle, i.e., with the expansion Mach number. The boundary layer has the effect of reducing the nozzle exit area. Such reduction would shift the calculated pressure ratio lines to higher Mach numbers. With the high primary Mach numbers required for the high pressure ratio the nozzle comes close to its expansion limit as seen from Fig. 12 (Appendix). The rapid change of the area ratio with the primary Mach number makes the analysis particularly sensitive to the accuracy of the input data for the area ratio.

For the analysis to be accurate it is quite important that the exact dimensions of the nozzle throat area, nozzle exit area and mixing section inlet area be entered in the calculation. Also the degree to which the cross-sectional area of the mixing section is maintained constant is important. For the agreement obtained here between experiment and analysis these dimensions were measured with an accuracy of better than $\pm$ 1%.

For the conditions shown in Figs. 4 and 5 the influence of the wall friction was minor in comparison to the influence of the geometric dimensions. A change by 10% in friction coefficient or length to diameter ratio is barely noticeable. This is essentially due to the low exit velocities for the conditions shown. However, if the already mentioned change in mixing mode occurs, which makes the mixing end velocity supersonic, wall friction can play a very determining role.

In Figs. 4 and 5 only the test points for which no mode change had occurred are entered. This restricts the test points to a region of low secondary Mach numbers, especially for higher ejector pressure ratios. The mode change at higher secondary Mach numbers adversely affects the ejector performance. This mode change and its influence will be discussed in detail in the next paragraph. In Sect IV it will be shown that the mixing mode change can be a beneficial factor in case of the optimized ejector featuring a tapered mixing section.

6. Mixing Mode Change

The change in mixing mode as experienced in the present experiments with constant area mixing for certain operating conditions is characterized by a transition from a rising to a more or less constant pressure distribution while primary flow and secondary flow undergo mixing. The beginning of the mode change, which occurs with either rising primary or secondary Mach number, is indicated by the appearance of a drop in static pressure at the beginning of the mixing process. If the mode change is completed, mixing occurs more or less at a pressure lower than the pressure prevailing at the inlet to the mixing section. Figure 7 shows typical pressure distributions for the transition from the normal to the changed mode condition. Though this transition occurs gradually with changing inlet conditions, the range of ejector operating conditions within which the mode change is completed is in general very small. For certain conditions it can occur fast enough to be regarded as a sudden change, distinctly noticeable in the noise level of the ejector. The mode change in the constant area mixing configuration exhibited practically no hysteresis (in contrast to the case of the optimized ejector, Sect. IV).

Analytical considerations allow the conditions for the occurrence of this mode change to be predicted. The prediction is based on a comparison of the ejector characteristics for constant area mixing with that for constant pressure mixing at a given ejector inlet geometry. Figure 8 gives the performance characteristics for

the conditions of the experimental ejector with the Mach number 2.7 primary nozzle with constant area mixing replaced by constant pressure mixing, which requires a variable area mixing section. In this characteristic the total ejector pressure ratio is plotted against the ratio of mixing section exit to inlet area necessary to accomplish constant pressure mixing (see Ref. 1). The plot is made up of curves for constant primary Mach number, secondary Mach number, and mass flow ratio. A point in this curve system fixes ejector inlet conditions. From the abscissa we can read, for given inlet conditions, the area reduction ratio "t" of the mixing section needed for constant pressure mixing. In particular we see that inlet conditions exist where this reduction ratio becomes unity, i.e., where constant pressure mixing requires a constant cross section area.

If we mark in Fig. 8 the inlet conditions where the experimental mode change occurred we are able to check how close the mode change comes to the line t = 1. This has been done in Fig. 8 with the two lines I-II and III-IV which correspond to the same designation in Figure 4. Along these lines in Fig. 8 the mode change occurs while the mass flow ratio is kept constant, in one case 4.3 in the other 20. We can see that in both cases the mode change occurs near or including the line t = 1. The mode change extends over a different range in each case. At the higher mass flow ratio the range is much shorter than at the lower ratio. Apparently where the constant pressure ratio curves run more or less parallel with the constant mass ratio curves, as can be seen in Fig. 4 for a mass ratio 4.3, the

mode change extends over a wider operating range than in the case where these two sets of curves cross at an angle as is the case for the higher mass ratio.

For the practical operation of the ejector the inlet conditions are controlled by the primary and secondary plenum pressures. To give an indication of how fast the mode change occurred in operating the ejector the ranges of primary pressure are given for the two indicated cases. At a mass ratio 4.3 the mode change occurred by raising the primary pressure form 145 to 147 psig, for a mass ratio 20 the mode change occurred by raising the primary pressure from 156 to 159 psig.

A very important factor in the phenomenon of the mode change is that it is strongly influenced by the wall friction conditions. For zero wall friction the whole diagram in Fig. 8 would fall below $t = 1$, i.e., no mode change would occur. Evidence for the wall friction influence is provided by tests with the square mixing section, for which the mode change occurred earlier (with rising secondary Mach number) than with the round mixing section. This follows since a square crossection, due to corner effects, is less favorable for the flow than a round one of equal cross-sectional area.

Under the prevailing conditions the change over to constant pressure mixing requires supersonic velocity at the end of the mixing process ("Supersonic mode"). Analytically this means that the supersonic solution of the mixing relations applies (see Ref. 1). It is obvious that due to the supersonic velocities the absolute

wall friction is higher than for the subsonic case. It is inherent to the constant area mixing process that the loss due to wall friction, which causes the coincidence of constant pressure and constant area mixing in the first place, cancels the gain in performance due to constant pressure mixing, i.e., there can be no change in performance due to mode change. However, to the degree the supersonic velocity is maintained after mixing and before supersonic diffusion takes place, performance deterioration occurs. This actually happens if the primary Mach number is increased beyond that required to cause the mode change, with the result that the ejector pressure ratio decreases after the mode change with increasing primary Mach number (at constant secondary mass flow).

In the next Section the case of the optimized ejector will show that the mode change in a decreasing area mixing section will lead to a performance improvement.

SECTION IV

EXPERIMENTS WITH THE OPTIMIZED EJECTOR

1. Ejector Layout

Figure 9 gives the layout of the optimized ejector. Its main feature is the tapered mixing section. The purpose of the tapered mixing section is to allow an increase of the secondary Mach number while mixing proceeds, providing, in this way, good mixing efficiency, (Reference 1).

As indicated before, the ejector layout is the result of the optimization procedure given in Reference 1. The design goal for the optimization was a total ejector pressure ratio of 5 at a mass flow ratio (primary to secondary) of 5. The optimization procedure provides the ejector inlet conditions, i.e., the layout of the primary nozzle, the primary to secondary inlet area ratio and the secondary Mach number. Flow data (wall friction and subsonic diffuser efficiency), the taper of the mixing section, and the character of the pressure distribution during mixing must be assumed to perform the optimization.

The flow data assumed for the initial optimization were of a preliminary nature and did not completely agree with the present experimental experience. For the comparison of analysis and experiment, shown in Figure 10, more realistic flow data were used in the analysis. The wall friction factor indicated in Figure 10 is a result of the experiments with the constant area ejector described

in the previous section. The indicated subsonic diffuser efficiency was determined from a flow survey at the entrance to the diffuser under the test condition of test point 4. Thus, the analytical performance shown in Fig. 10 is based on very realistic assumptions for wall friction and subsonic diffuser efficiency.

For the taper of the mixing section, as given by the area ratio between exit and entrance cross sections, a value of t = .7 was chosen. This choice was made under the assumption that the exit flow is subsonic and under the consideration that the taper should be short of causing sonic flow in the exit. Since the appearance of sonic flow in the exit depends on both the taper, and on the unknown character of the pressure distribution during mixing, the choice of the taper becomes quite arbitrary. We will see later that the insight gained from the experiments allows one to remove this arbitrariness to a significant degree.

The character of the pressure distribution during mixing which must be assumed for the optimization process is difficult to predict. The assumptions made in the design of the present ejector were not confirmed by the experiments as will be explained in more detail later. The consequence is that the geometry of the present ejector is not exactly that for optimum performance although in a first approximation the optimization remains valid. This deviation from an optimized geometry is immaterial for comparing experimental and analytical performance, since the comparison is done on the basis of a given ejector geometry. Fig. 10 gives the performance of the

"optimized" ejector with the revised flow data. The analysis expresses the character of the pressure distribution during mixing in terms of a pressure distribution factor i. A zero value for i indicates constant pressure mixing, a value of unity applies to a near straight rise in pressure during mixing up to a defined value at the mixing section exit (for an exact definition of i see Sec. IV 3).

Fig. 10 gives a choice of performance curves for the ejector pressure ratio of 5 based on different distribution factors i. An apparent design point for optimum performance can be determined from the diagram. It is characteristic for the optimum design point that the design mass flow ratio and the pressure ratio curve are tangent to each other at this point. This is the case for an i-value of .82. In the original optimization process an i-value of .6 had been assumed. In the following section the performance and the i-value will be compared with experimental values.

2. Design Point Performance

In Fig. 10 five test points are entered which have measured total ejector pressure ratios of 5. They only differ by their mass flow ratios which are indicated by the analytical mass flow ratio curves. In the following discussion we will see that the test points also differ in the character of their pressure distribution during mixing. Test points 4 and 5 readily meet the design point performance. Of special interest here is that test points 4 and 5, in

contrast to test points 1 to 3, are in the "supersonic mode" condition experienced previously with the constant area ejector. The mixing mode transition occurred quite suddenly and was accompanied by a rise in performance. This is in contrast to the experience with the constant area mixing case where no change in performance occurred during the mixing mode change. The obvious reason is that only with a tapered mixing section can the wall pressure forces, which are a function of the pressure distribution, change and influence the ejector performance. The mode change with the optimized ejector also exhibited some hysteresis. Test point 4 was obtained just after the mode change had occurred with rising primary pressure and test point 5 just before the mode change was reversed with falling primary pressure. Despite the difference in primary pressure both points have the same ejector pressure ratio. The significance of this fact will be discussed below.

3. Pressure Distribution

In Figure 11 the static pressure distributions extending along the mixing section and the supersonic diffuser are plotted for the 5 test points marked in Figure 10. To determine the i-value characterizing these pressure distributions each curve will be compared with the idealized distribution curves given by the two straight inclined lines in Fig. 11. These lines represent pressure distributions for which the factor i is close to unity, with the dashed line pertaining to cases 1 to 3 and the solid line to cases 4 and 5.

This follows from the definition of i (see Ref. 1), which states that i is unity if the pressure in the mixing section rises proportionally with the change in cross-sectional area along the mixing section. For a converging, cone-shaped mixing section with a small taper the resulting pressure distribution is very nearly a straight line. For the subsonic solution of the ejector equations as used here, in case of i = 1, mixing and shock-diffusion are completed at the mixing section exit.

Taking the inlet pressure as a base value, the area underneath any other pressure distribution curve within the tapered mixing section is an approximate measure for the i-value belonging to this curve. In this way the curves 1, 2, 3, 4, and 5 in Figure 11 can be assigned approximate i-value of 1, .6, .5, .1, and .1, respectively. If we compare these i-values with those obtained from the location of the test points in Figure 10 we find in both cases the i-values decrease with increasing secondary Mach number. However, the real i-values obtained from Figure 11 are lower than those determined from the analysis. In particular, the design performance has been obtained with an i-value of .1, i.e., under near constant pressure mixing conditions, instead of i = .82 as found by the analysis. If one checks the analytical performance in Fig. 10 for i = 0.1, one finds that it is superior to the experimental performance. The following consideration provides an explanation for this discrepancy. From the pressure distribution curves 4 and 5 in Fig. 11 one recognizes that the shock diffusion in the supersonic diffuser is appre-

ciably delayed. This can be taken as an indication that mixing extends into the supersonic diffuser. This conclusion is supported by a total pressure survey of the flow in the supersonic diffuser, which revealed a quite pointed flow profile in the entrance of the diffuser. If one assumes that the mixing process requires the length of the tapered mixing section but is delayed and actually shifted downstream 1/3 the length of the mixing section into the constant area supersonic diffuser, then the effective taper for the mixing process is 0.8 rather than 0.7. The pressure distribution factor required by the analysis in this case to obtain the design point in Figure 10 would have to be i = 0, i.e., a constant pressure distribution is required, which is in close agreement with the experimental result.

The present test results have important consequences for the optimization process. They have shown that optimum performance is obtained in the supersonic mode, characterized by near constant pressure mixing conditions. As already experienced in the constant area mixing experiments the supersonic mode is very stable and unaffected by the primary pressure, once it is established. This can again be seen by comparing the pressure distribution curves of test point 4 and 5 in Fig. 11. Only the supersonic shock diffusion is moved downstream with an increase in primary pressure (from 5 to 4). For both test points the ejector pressure ratio is the same, only the mass flow ratio is different due to the difference in primary pressure. The significance of this result is that the optimization process

can assume the pressure distribution as known, namely that of constant pressure independent of the required taper. The taper now becomes a result of the optimization and optimum operating conditions found are always in agreement with the required mode change conditions demonstrated in Sect. III 6 for the constant area mixing case.

The ability to prescribe a realistic pressure distribution for the optimization removes the arbitrariness from the optimization process of Ref. 1 caused by the free choice of both the taper and the character of the pressure distribution. Preliminary analytical results for the optimization under constant pressure mixing conditions indicate that the performance obtained is not necessarily better; however, as seen from above discussions, it reflects a more realistic condition and should therefore be more reliable than the original optimization procedure.

SECTION V

CONCLUSIONS

The "basic ejector," which omits the subsonic diffuser and has a constant area mixing section of sufficient length to assure complete mixing is a very suitable instrument to check the basic validity of an ejector analysis. It provides very well defined conditions for the comparison of analysis and experiment. The findings with the basic ejector experiments are, that for a primary nozzle laid out for Mach number 2.7, the agreement between experiment and analytical prediction is quite satisfactory over the test range, which extended for the ejector total pressure ratio from 3 to 5 and for the mass flow ratio, primary to secondary, from infinite to 4 and 12, respectively. Lower values for the mass flow ratio cause an all supersonic mixing mode which in the case of constant area mixing leads to performance deterioration. This mixing mode change is an important factor in the case of a decreasing area mixing section, as will be discussed below. There is practically no difference in performance when changing from a round to a square mixing section while maintaining the same cross-sectional area.

The experiments with the basic ejector featuring a primary nozzle designed for Mach number 3.2 gave somewhat less satisfactory agreement between experiment and analysis. A likely reason is the nature of the primary nozzle which had a straight conical contour for its supersonic expansion region. The radial component produced

by this contour was not accounted for in the analysis. The Mach number 2.7 primary nozzle which gave near perfect agreement was of the same conical design. The effect of the conical nozzle apparently increases with the design Mach number. The ejector pressure ratio range covered by the experiments with the Mach number 3.2 nozzle was from 4 to 7 with the mass flow ratio reaching from infinity to 6 and 20, respectively. Again, a mixing mode change occurred for lower mass flow ratios. The largest deviation between experiment and analysis occurred for the ejector pressure ratio seven. For instance, at a mass flow ratio of 40, the analysis requires a primary Mach number of 3.49, the actual Mach number calculated from the experimental data being 3.56. For smaller mass flow ratios the difference decreased somewhat.

The mixing mode change occurred with rising secondary mass flow, occurring earlier the higher the ejector pressure ratio. It can be predicted analytically. It occurs for the condition where constant pressure mixing requires a constant area mixing section. The important factor is that this condition is a strong function of the wall friction in the mixing section. Theoretically no mode change can occur in a constant area mixing section for zero wall friction. However, a mode change can occur without friction in a tapered, i.e., decreasing, area mixing section. This is important for an "optimized ejector," which must have a tapered mixing section to obtain a maximum of performance under the prevailing conditions of the high primary Mach number ejector.

In contrast to the constant area mixing case, the performance of the ejector with a tapered mixing section improves markedly with a change to the supersonic mixing mode. It was under such conditions that the optimized ejector reached its design goal of a total pressure ratio of 5 at a mass flow ratio (primary to secondary) of 5. The original optimization of this ejector did not take a mode change into account, choosing, instead, a pressure distribution with a strong pressure rise which is characteristic for the unchanged mode believed to be applicable in this particular case. The experiments showed that the supersonic mode was the only one possible in the regime of optimized performance. The experiments further revealed that the character of the pressure distribution in the supersonic mode was the same in all cases, whether the mixing section was tapered or not, namely, that of near constant pressure. This is an important finding, since it allows the optimization process to be simplified. Constant pressure mixing can be assumed and, hence, the required taper of the mixing section becomes a result of the optimization. The original optimization had to make assumptions about the pressure distribution as well as about the taper.

The "off design" operation of the primary nozzle, i.e., the operation of the primary nozzle with a Mach number higher than its design Mach number, can be very satisfactorily accounted for in the analysis by a momentum conservation consideration for the flow expanding outside the nozzle, as shown in the Appendix.

APPENDIX

FLOW RELATIONS FOR OFF-DESIGN NOZZLE

This analysis treats only the case in which the flow further expands outside the nozzle, i.e., the final expansion Mach number is larger than the nozzle design Mach number. In the absence of wall forces outside the nozzle the gain in momentum in the nozzle direction by the expanding flow simply equals the pressure forces acting on the flow at the nozzle exit. The total axial momentum of the flow after complete expansion is therefore:

$$\dot{m} \cdot V_p = V_{noz} \cdot \dot{m} + A_{noz}(P_{noz} - P_p) \tag{1}$$

Using the following basic relations:

$$\dot{m} \cdot V = A \cdot p \cdot \gamma \cdot M^2 \tag{2}$$

$$\dot{m} = A \cdot \rho \cdot V \tag{3}$$

or with $$a = \sqrt{R \cdot \gamma \cdot T} \tag{4}$$

$$\dot{m} = A \cdot p \cdot M \frac{\gamma}{\sqrt{R \cdot \gamma \cdot T}} \tag{5}$$

we can write:

$$P_{noz} \cdot M_{noz} \cdot \gamma \frac{V_p}{\sqrt{R \cdot T_{noz} \cdot \gamma}} = P_{noz} \cdot \gamma \cdot M_{noz}^2 + (P_{noz} - P_p) \tag{6}$$

or

$$M_{noz} \cdot \gamma \cdot M_p \sqrt{\frac{T_p}{T_{noz}}} = \gamma \cdot M_{noz}^2 + 1 - \frac{P_p}{P_{noz}} \tag{7}$$

then $$\frac{P_p}{P_{noz}} = \gamma \cdot M_{noz}^2 + 1 - \gamma \cdot M_{noz} \cdot M_p \sqrt{\frac{T_p}{T_{noz}}} \tag{8}$$

We can write for the temperature ratio in this equation:

$$\frac{T_p}{T_{noz}} = \frac{T_p}{(T_p)_0} \frac{(T_p)_0}{T_{noz}} \tag{9}$$

Since only the kinetic energy of the axial flow component is preserved in this expansion process the adiabatic expansion relations allow us to write:

$$\frac{T_p}{T_{noz}} = \frac{1 + M_p^2 \frac{\gamma-1}{2}}{1 + M_{noz}^2 \frac{\gamma-1}{2}} \tag{10}$$

Since in the ejector analysis we are interested in the overall pressure ratio of the complete expansion process we introduce this pressure ratio by writing:

$$\frac{P_p}{P_0} = \frac{P_p}{P_{noz}} \frac{P_{noz}}{P_0} \tag{11}$$

or $$\frac{P_p}{P_0} = \frac{P_p}{P_{noz}} \left(1 + \frac{\gamma-1}{2} M_{noz}^2\right)^{\frac{\gamma}{\gamma-1}} \tag{12}$$

With Eqs. (10) and (11) we can write for the overall pressure ratio of the expansion process for an "off design" nozzle:

$$\frac{P_p}{P_0} = \frac{\gamma \cdot M_{noz}^2 + 1 - \gamma \cdot M_{noz} \cdot M_p \sqrt{\frac{1 + M_{noz}^2 \frac{\gamma-1}{2}}{1 + M_p^2 \frac{\gamma-1}{2}}}}{\left(1 + \frac{\gamma-1}{2} M_{noz}^2\right)^{\frac{\gamma}{\gamma-1}}} \tag{13}$$

This relation can be also readily solved for the final flow Mach number of the expansion:

$$M_p^2 = \frac{Z^2}{1 + \left(M_{noz}^2 - Z^2\right) \frac{\gamma-1}{2}} \tag{14}$$

where

$$Z = \frac{1 + \gamma \cdot M_{noz}^2 - \frac{p_p}{p_o}\left(1 + \frac{\gamma-1}{2} M_{noz}^2\right)^{\frac{\gamma}{\gamma-1}}}{\gamma \cdot M_{noz}} \tag{15}$$

We can readily derive the area ratio for the expansion outside the nozzle area to the flow cross section area of the totally expanded flow. With the continuity law it is:

$$\rho_{noz} \cdot v_{noz} \cdot A_{noz} = \rho_p \cdot v_p \cdot A_p \tag{16}$$

using again Eq. (4) and applying the equation of state:

$$\rho = \frac{p}{R \cdot T} \tag{17}$$

we can write:

$$\frac{A_{noz}}{A_p} = \frac{p_p}{p_{noz}} \quad \frac{M_p}{M_{noz}} \sqrt{\frac{T_{noz}}{T_p}} \tag{18}$$

With Eq. (8) we can also write:

$$\frac{A_{noz}}{A_p} = \left(\gamma \cdot M_{noz}^2 + 1 - \gamma \cdot M_{noz} \cdot M_p \sqrt{\frac{T_p}{T_{noz}}}\right) \frac{M_p}{M_{noz}} \sqrt{\frac{T_{noz}}{T_p}} \tag{19}$$

or:

$$= M_p \left[\left(\gamma M_{noz} + \frac{1}{M_{noz}}\right)\sqrt{\frac{T_{noz}}{T_p}} - \gamma M_p\right] \tag{20}$$

introducing Eq. (10) yields

$$\frac{A_{noz}}{A_p} = M_p \left[\left(\gamma \cdot M_{noz} + \frac{1}{M_{noz}}\right)\sqrt{\frac{1 + M_p^2 \frac{\gamma-1}{2}}{1 + M_{noz}^2 \frac{\gamma-1}{2}}} - \gamma M_p\right] \tag{21}$$

Since the throat to exit area ratio of the nozzle itself is given by the well known relation:

$$\frac{A^*}{A_{noz}} = \left(\frac{\gamma+1}{2}\right)^{\frac{\gamma+1}{2(\gamma-1)}} \cdot M_{noz}\left(1 + \frac{\gamma-1}{2} M_{noz}^2\right)^{-\frac{\gamma+1}{2(\gamma-1)}} \qquad (22)$$

the nozzle throat to final expansion area for the off-design flow can be determined from:

$$\frac{A^*}{A_p} = \frac{A_{noz}}{A_p} \cdot \frac{A^*}{A_{noz}} \qquad (23)$$

The analysis of Ref. 1 assumes equal static pressure for primary and secondary flow at the inlet to the mixing section. If one assumes that no essential mixing takes place, while the primary flow is expanding to its final pressure outside the nozzle, i.e., to the pressure of the secondary flow, an inlet area ratio for off-design conditions can be defined:

$$\frac{A_p}{A_s} = \frac{A_p}{A_{noz} + (A_s)_{geo} - A_p} \qquad (24)$$

since

$$A_{noz} = (A_p)_{geo}$$

$$\frac{A_p}{A_s} = \frac{1}{\frac{A_{noz}}{A_p}\left[1 + \left(\frac{A_s}{A_p}\right)_{geo}\right] - 1} \qquad (25)$$

In this equation A_{noz}/A_p is determined from M_p by Eq. (21), and $(A_s/A_p)_{geo}$ is given by the ejector design. For off-design conditions the inlet area ratio of the ejector as defined by the analysis is a variable for a given ejector, depending on the primary inlet Mach number chosen. For calculating an ejector characteristic as given in Fig. 4 or 5, an iterative process is necessary to properly correlate primary Mach numbers and inlet area ratios.

To demonstrate the influence of an off-design nozzle on the expansion process, the area and pressure ratios associated with the two primary nozzles used in the present experiments are plotted in Fig. 12 against the final expansion Mach number. For comparison, the area and pressure ratio for the ideal supersonic nozzle are also entered. The plot shows that the deviations from ideal conditions beyond Mach numbers 2.7 and 3.2, respectively, are at first only slight. However, beyond Mach number 3.1 and 3.6, respectively, the deviations from ideal conditions get out of bounds very fast. It is also obvious that for each nozzle a barrier is reached beyond which practically no ejector operation is possible, i.e., increasing the primary pressure hardly changes the primary Mach number. Also for the present ejector geometries the inlet area ratio increases rapidly to very high values at this point.

REFERENCE

1. Hasinger, S., "Performance Characteristics of Ejector Devices", former Aerospace Research Laboratories, Wright-Patterson AFB, Technical Report ARL TR-75-0205, June 1975.

ERRATA TO REFERENCE 1

p. 11 add +1 at the left side of Eq. (9a)

p. 16 the denominator on the right side of Eq. (21c), outside the root, should read: $B_\tau \; t \; [(A_p/A_s) + 1]$

p. 37 Eq. (77) should read: $c_p = \gamma \; R_{Ex}/(\gamma_{Ex} - 1)$

p. 51 delete factor 2 in nominator of Eq. (111)

p. 52 Eq. (116) should read: $A_s/A_p = (B + \sqrt{B^2 + 4AC})/2A$

p. 53 Eq. (109a) should read: $a_2 = -t \; \tau/\gamma_p$

Above corrections concern misprints and in no way affect the calculations of the report. To clarify the text the following corrections should be made:

p. 15 The second sentence after Eq. (37) should read: If the pressure rises proportionally with the change in mixing section cross sectional area the factor i is one.

p. 17 last paragraph should end: ...entering flow can be determined (for $\gamma = 1.4$):

p. 21 line 4 and 5 in text after Eq. (47) should read: ...approximate value for M_{Ex} with Eqs. (9), (5), (21), (16a) and (22). This...

p. 21 after second paragraph (ending with ...overcomes this problem) insert the following paragraph:

In the present case it is advantageous for the conversion process to solve Eq. (9) for M_p^2 (carrying M_s as independent variable:

$$M_p^2 = \frac{1 + (A_p/A_s)}{\gamma_p \, A_p/A_s}\left[f \frac{(p_{Ex})_0}{p_s} - \gamma_s M_s^2 \left(\frac{1}{1 + (A_p/A_s)} - \frac{c_f \ell}{2d} \right) - 1 \right]$$

p. 52 the second sentence after Eq. (116) should read: ...an improved f-value can be determined with the help of Eqs. (21), (16a), (22), and (47).

p. 53 After Eq. (109a) add:

In abbreviated form Eq. (105) becomes

$$M_p^2 = ((1 + A_p/A_s)a - b)/(A_p/A_s) \qquad (105a)$$

Use Eqs. (21c), (16a), (22c), and (57) to obtain an improved f_τ-value.

p. 68 in the caption of Figure 4 the title should read: Flow density Parameter E_τ for $c_f \ell/(2d) = 0$

p. 77 5th notation from top in Figure 11a should read: c_{p-s}/c_{p-p}

p. 88 in Fig. 21a the curve parameters 10 and 20 should be switched in lower set of curves.

p. 108 change denominator in notation for parameter P_s from $M^2 \gamma$ to $M_s^2 \gamma_s$

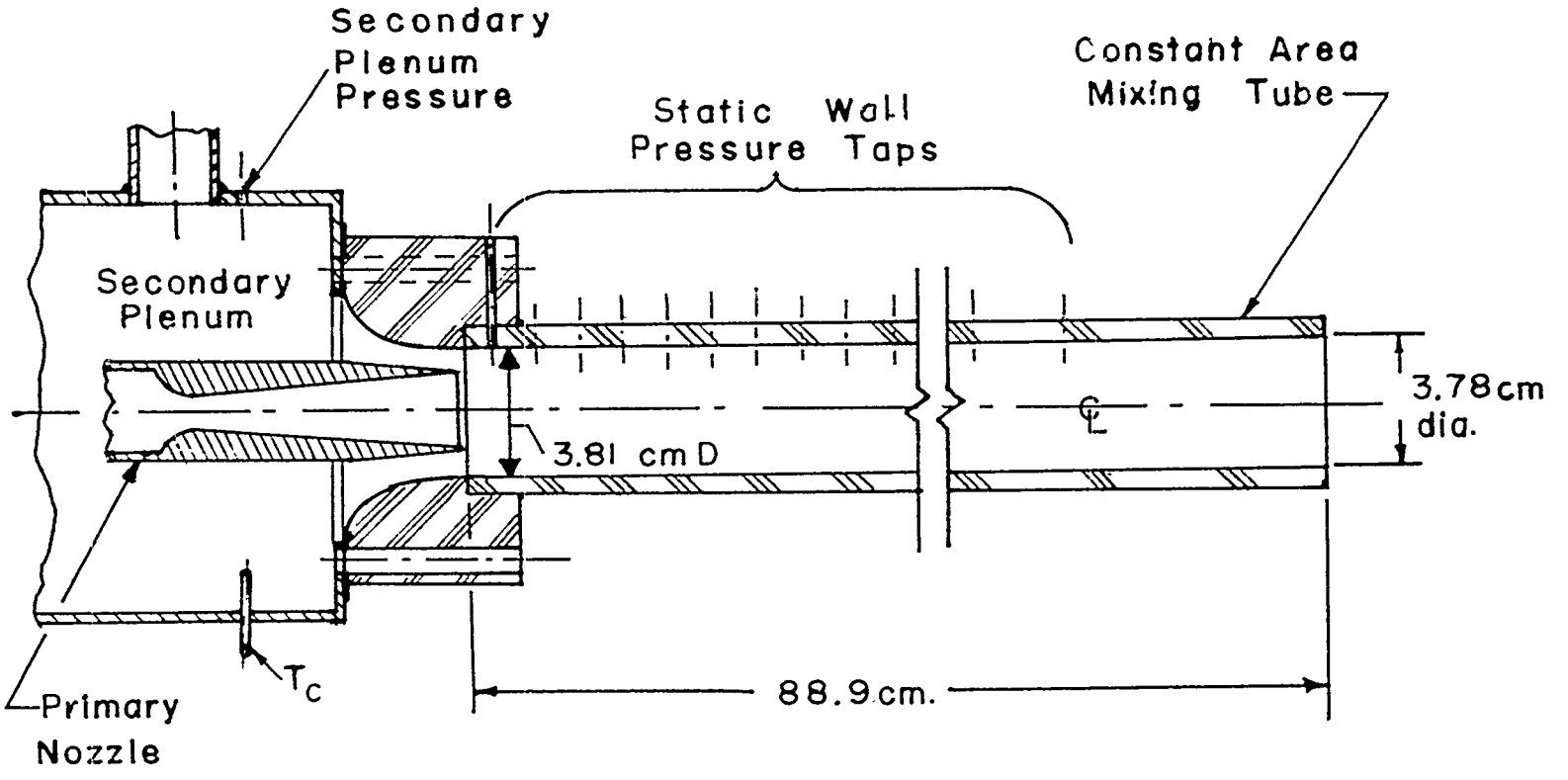

Figure 1 Layout of the Ejector Used in the Basic Ejector Experiments Featuring a Constant Area Mixing Section, which also Serves as Supersonic Diffuser. There is no Subsonic diffuser.

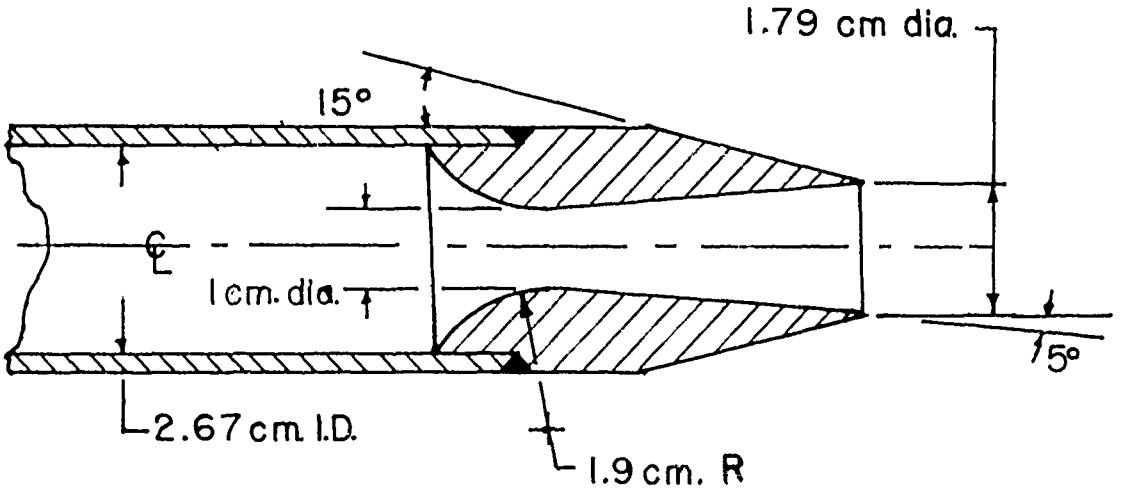

M 2.7 NOZZLE

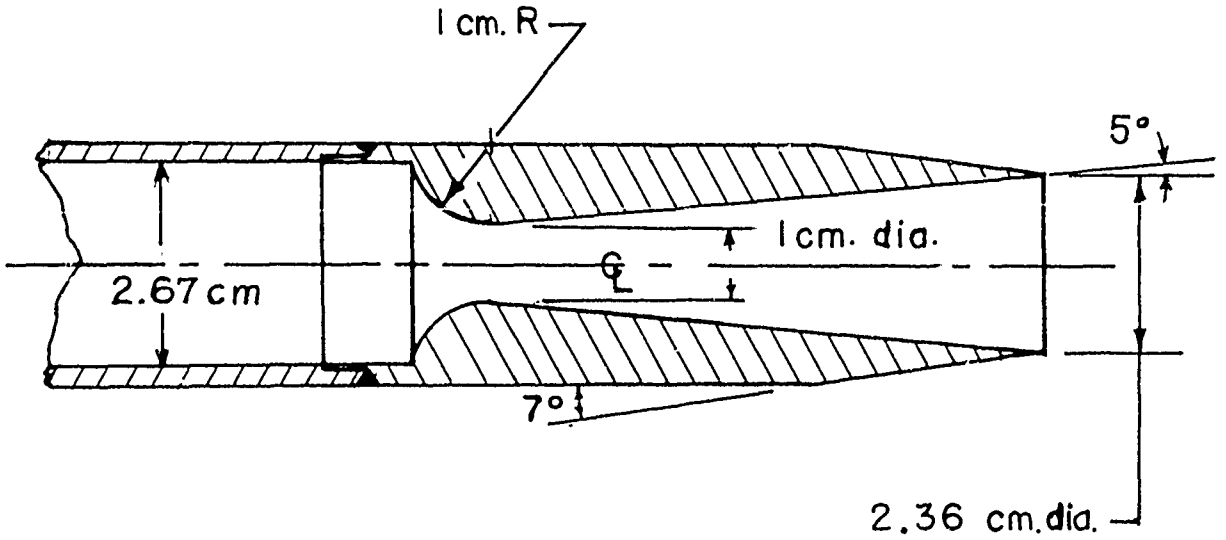

M 3.2 NOZZLE

Figure 2 Primary Nozzles Used in the Experiments.

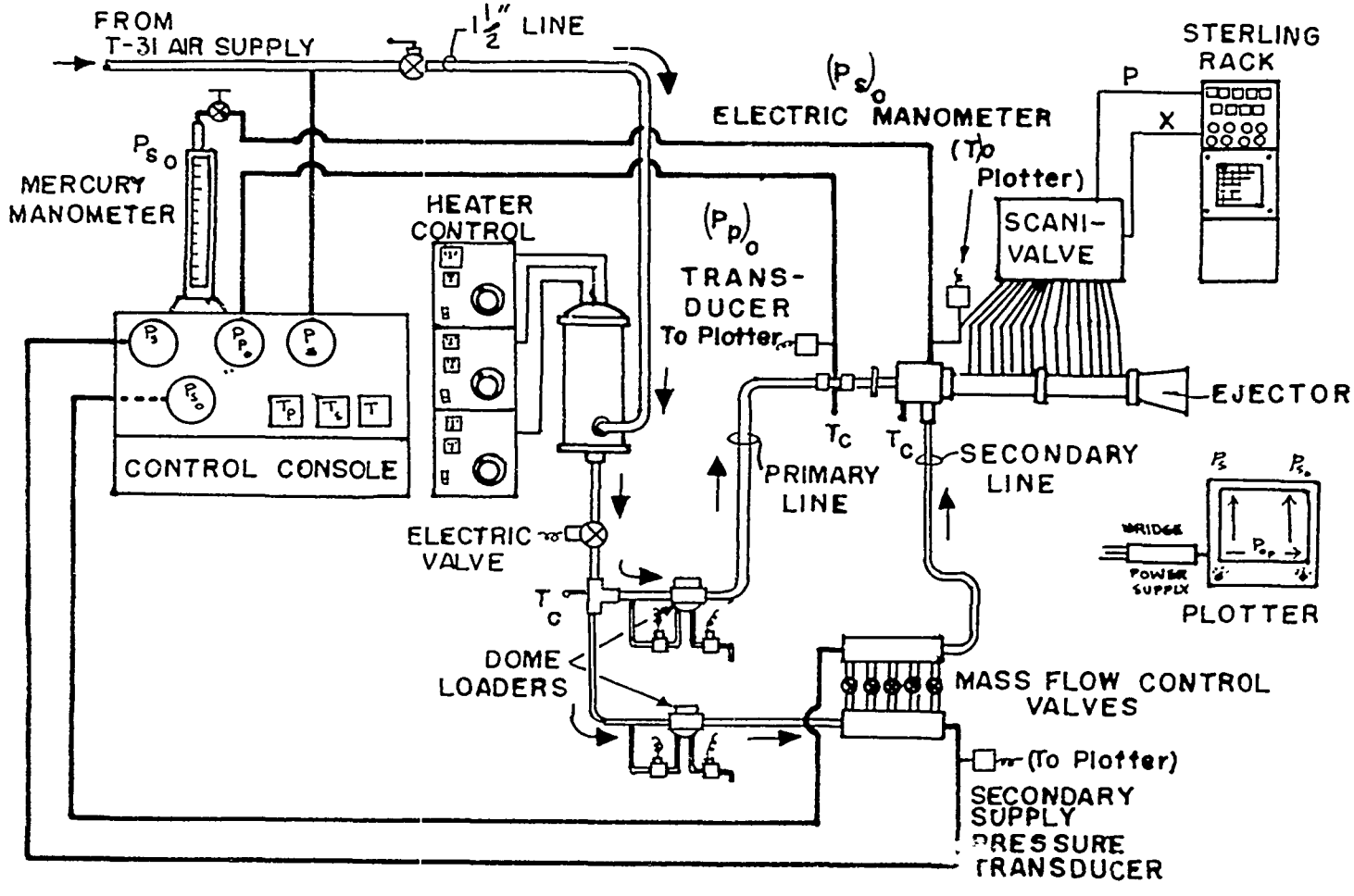

Figure 3 Layout of the Ejector Test Stand.

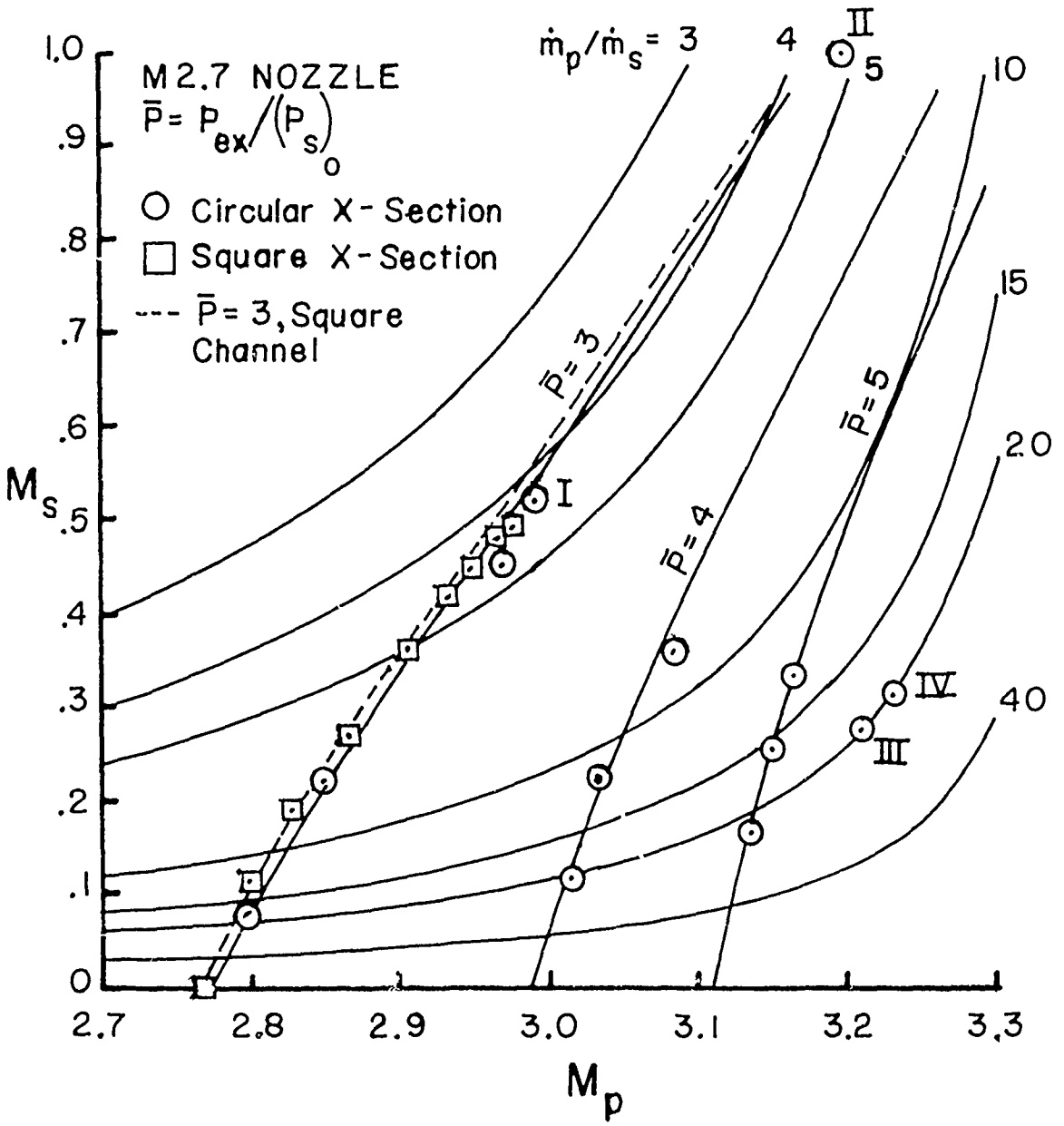

Figure 4 Comparison of Analytical and Experimental Performance of the Basic Ejector with the Mach Number 2.7 Primary Nozzle. (For test points marked by roman numerals see Section III 6)

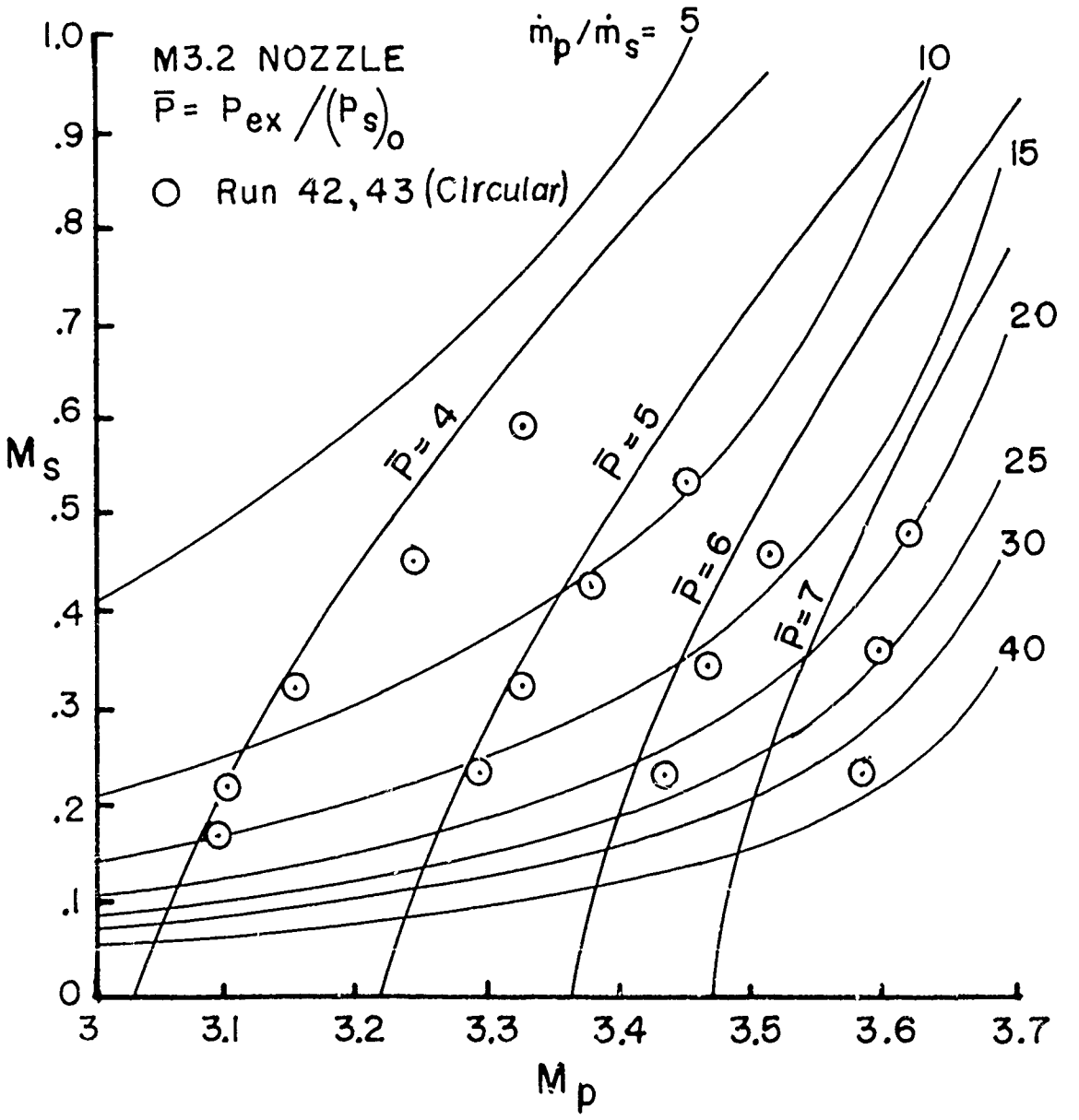

Figure 5 Comparison of the Analytical and Experimental Performance of the Basic Ejector with the Mach Number 3.2 Primary Nozzle.

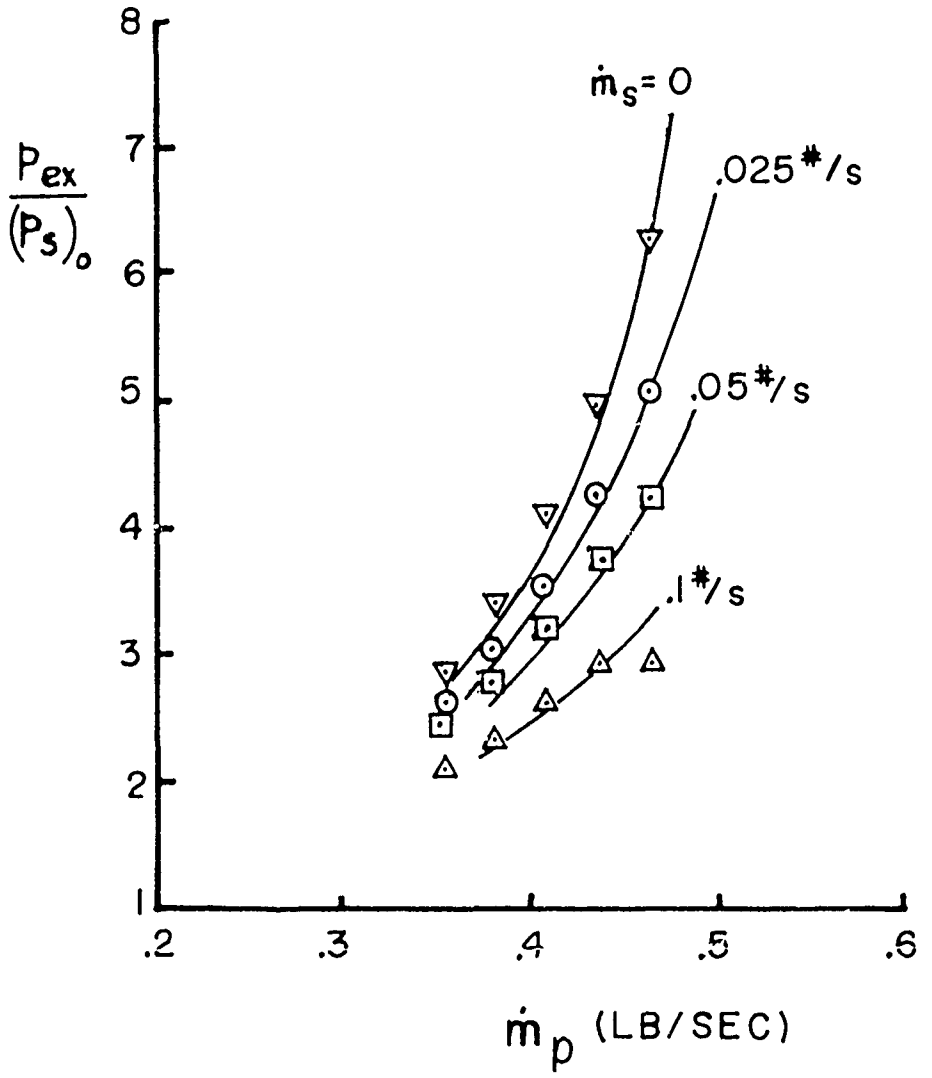

Figure 6 Performances Shown in Figure 4 Presented in Terms of the Absolute Primary and Secondary Mass Flows.

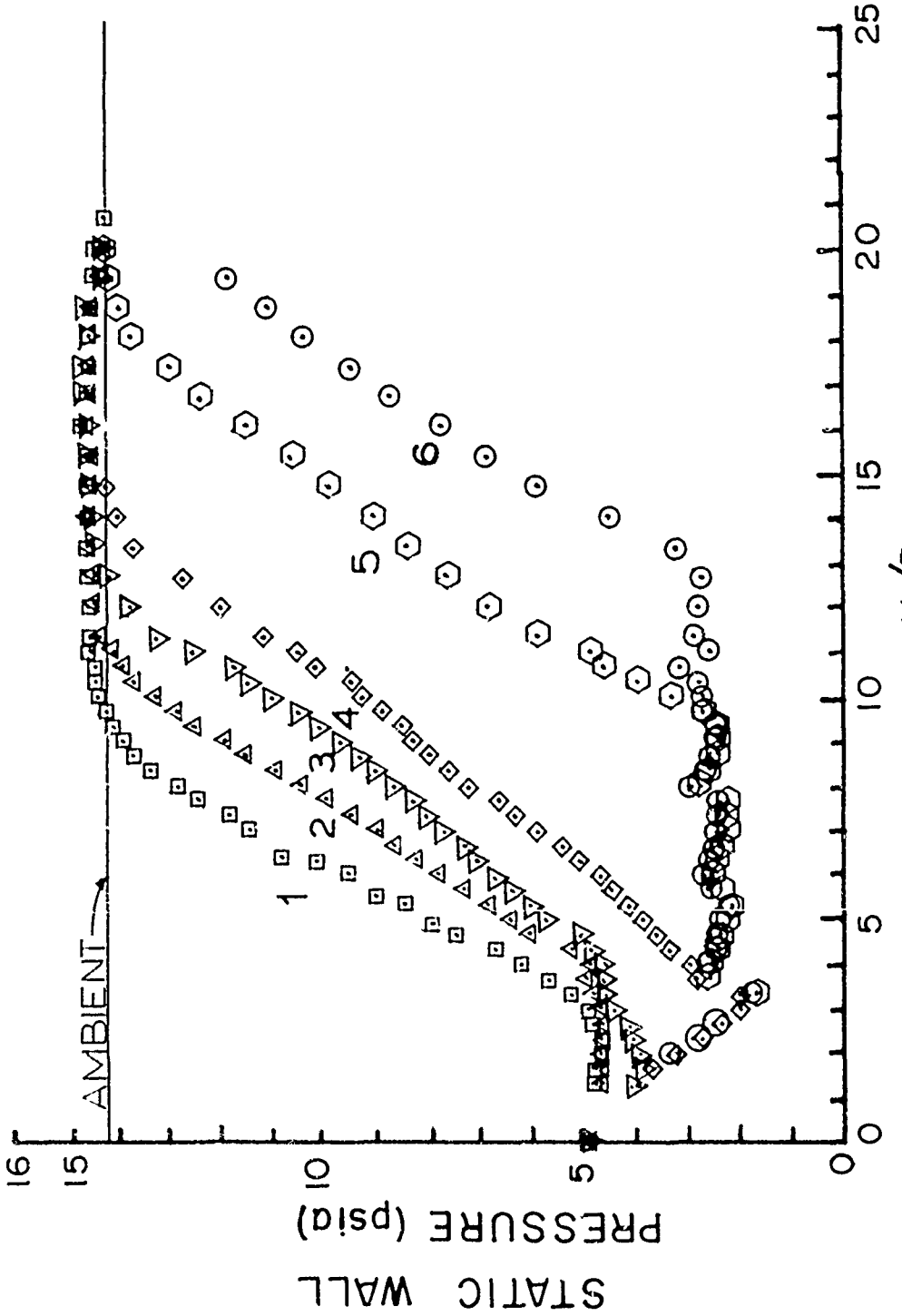

Figure 7 Typical Static Pressure Distributions Along the Mixing Section of the Basic Ejector for Regular and Changed Mixing Mode Conditions. (Curves 1 to 3 before mode change with secondary Mach number increasing from 1 to 3, curves 4 to 6 after mode change with primary Mach number increasing form 4 to 6)

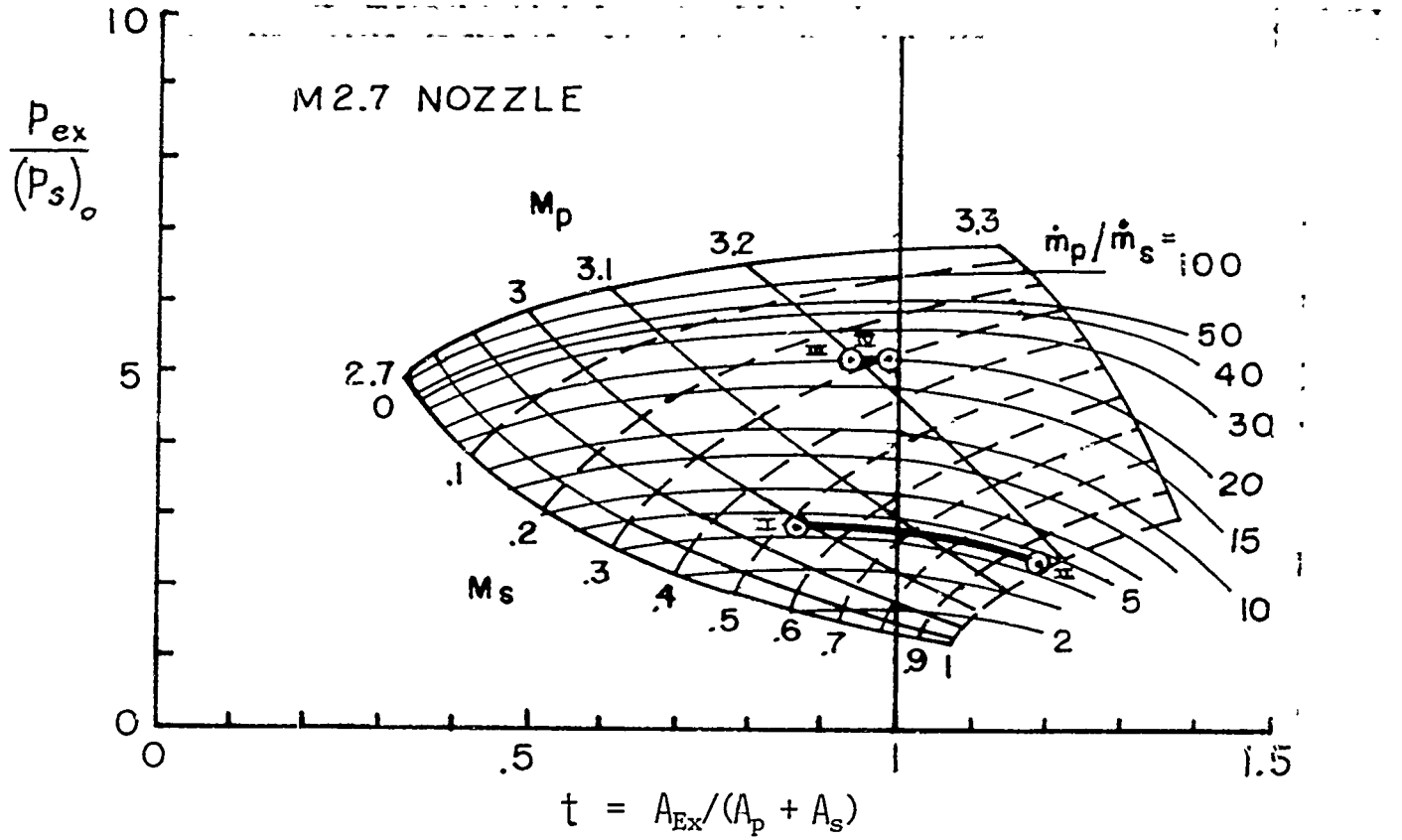

Figure 8 Performance Characteristic of the Experimental Ejector under the Assumption of a Converging Mixing Section with its Area Reduction Ration t Always Adjusted for Constant Pressure Mixing. Points I, II and III, IV, mark inlet conditions between which a mixing mode change occurred in the actual ejector.

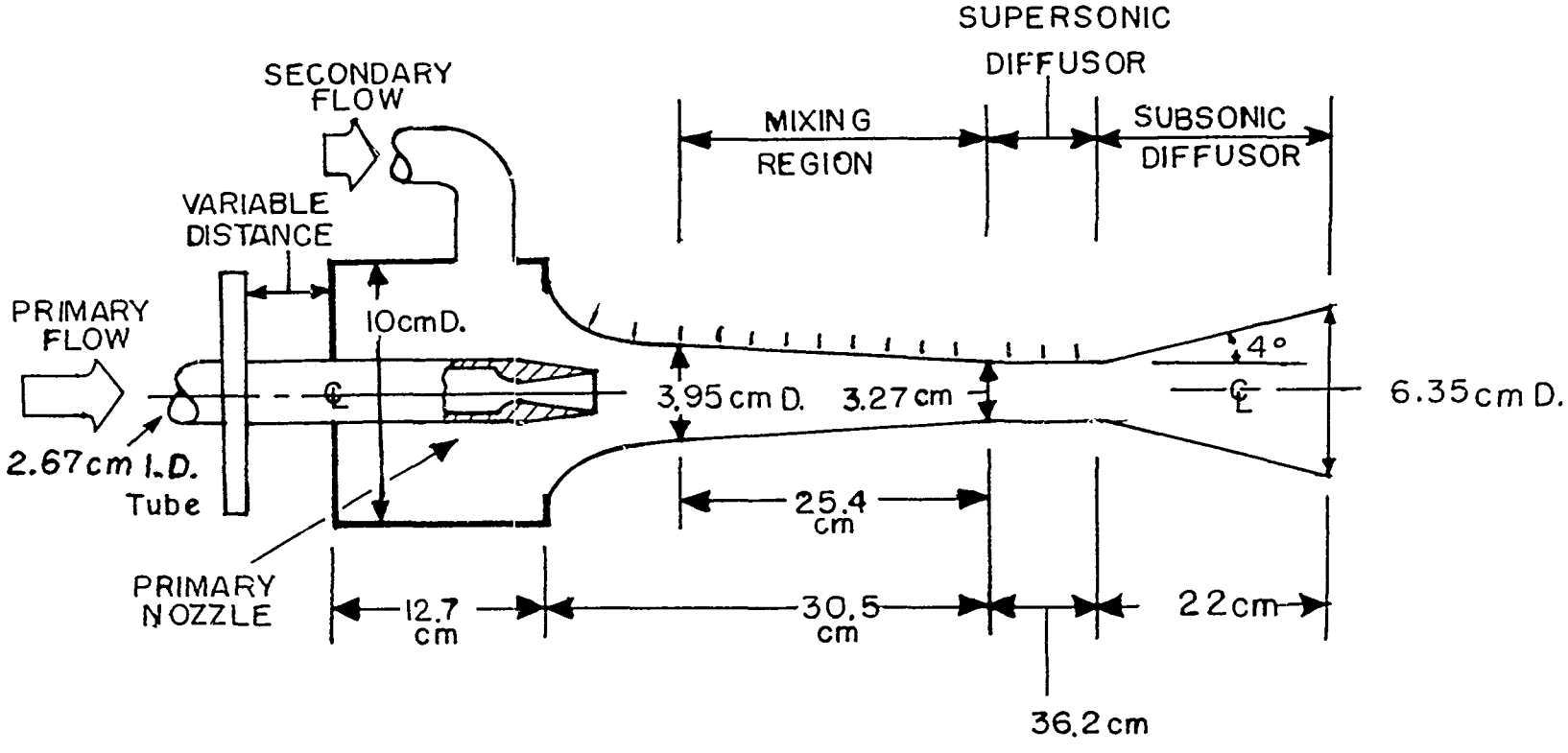

Figure 9 Layout of the Optimized Ejector (not to scale).

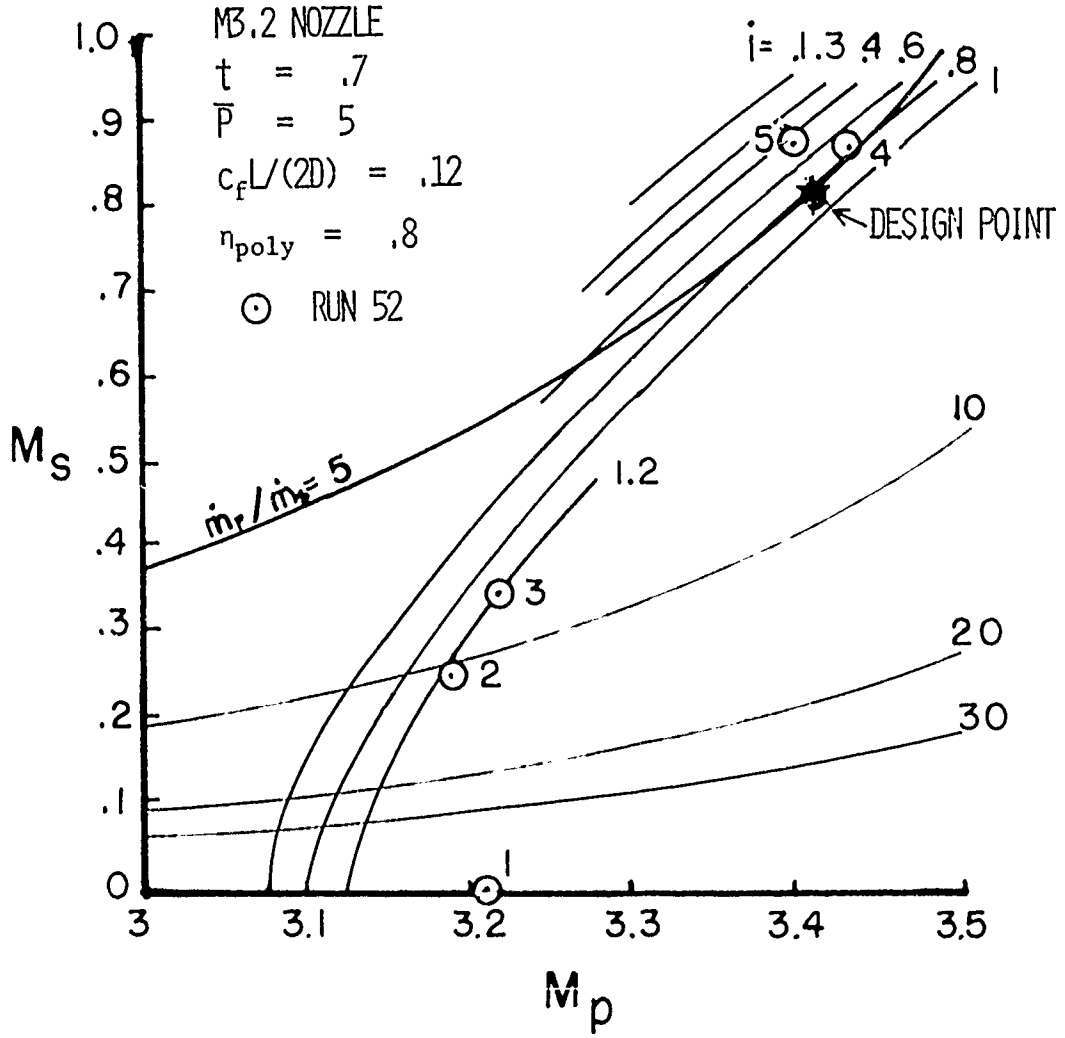

Figure 10 Comparison of the Analytical and Experimental Performance of the Optimized Ejector for a Total Pressure Ratio of 5 with the Pressure Distribution Factor i as Parameter.

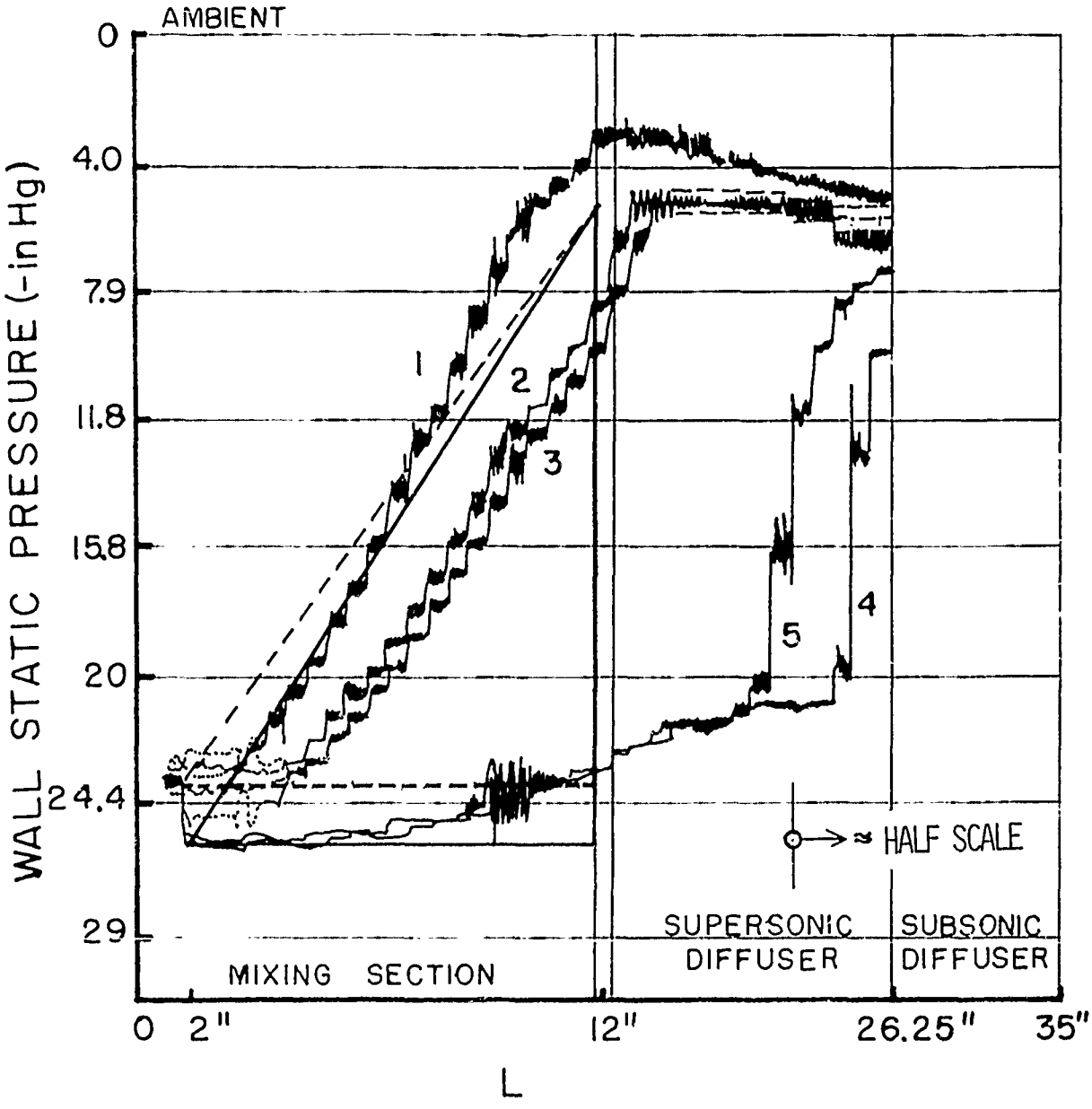

Figure 11 Static Pressure Distributions Along the Mixing Section and the Supersonic Diffuser of the Optimized Ejector for the Test Points indicated in Figure 10.

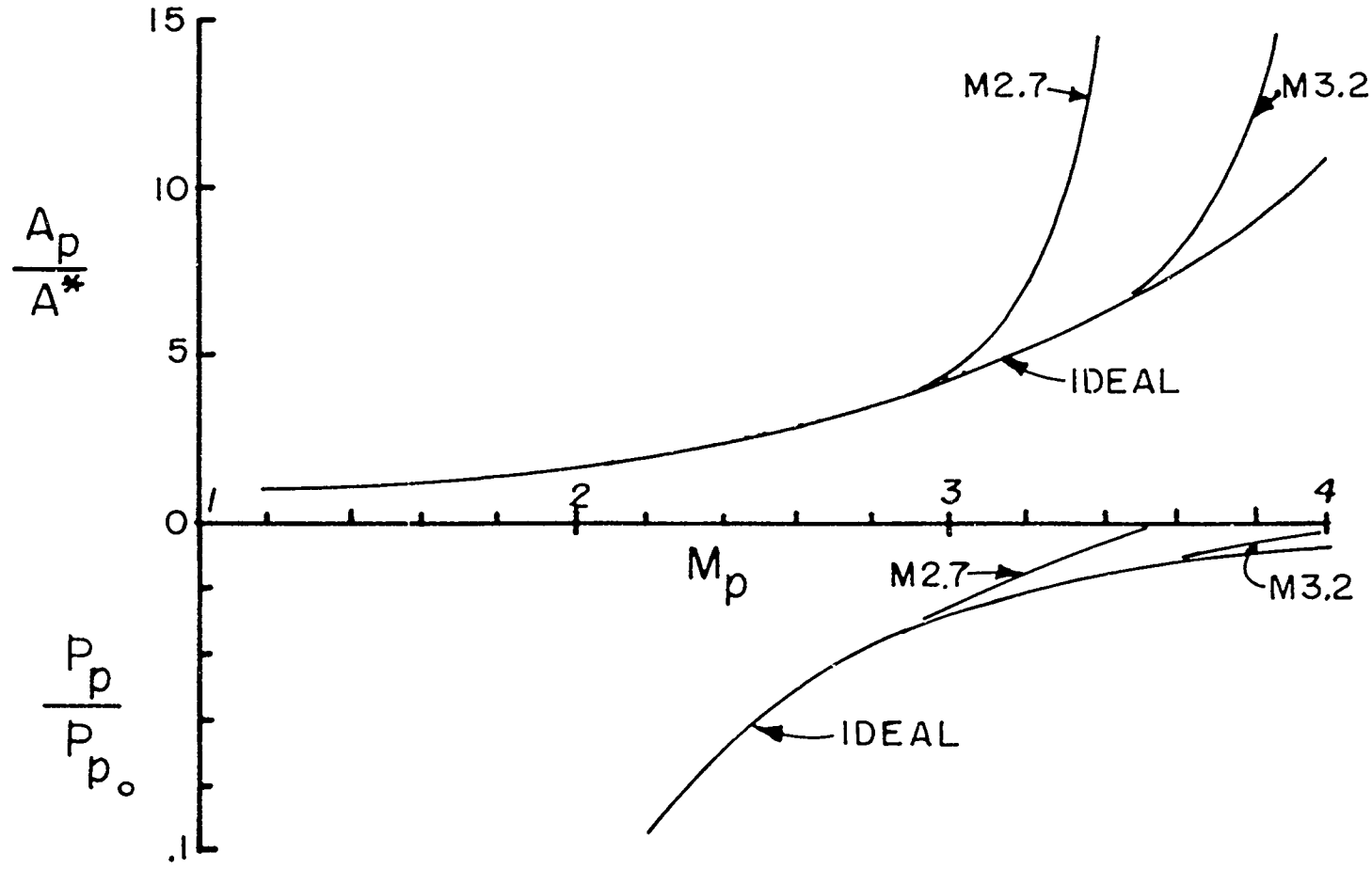

Figure 12 Area Expansion Ratio and Expansion Pressure Ratio for the ideal (Isentropic) Supersonic Nozzle and for the Nozzles actually used in the Present Experiments as Function of the Final Expansion Mach number, as derived under one-dimensional flow assumptions.